



Element differential method for free and forced vibration analysis for solids

Jun Lv, Chang Song, Xiao-Wei Gao*

State Key Laboratory of Structural Analysis for Industrial Equipment, Dalian University of Technology, Dalian 116024, China



ARTICLE INFO

Keywords:

Element differential method (EDM)
Elastodynamic problems
Free and forced vibration
Lagrange isoparametric elements
Collocation technique
Lumped mass matrix

ABSTRACT

In this work a new strong-form numerical method, element differential method (EDM), is proposed to perform free and forced vibration analysis of elastodynamic problems. The present method establishes the global algebraic system equations directly based on the strong form of the equilibrium equations without using any variational principles or energy principles. In this method, the isoparametric elements with a node inside them are utilized to discrete the geometries. And the direct differentiation of their shape functions is used to characterize the geometry and physical variables. A novel collocation technique is then proposed to generate the system of equations, in which the dynamic equilibrium equations are collocated only at the internal nodes of elements, and the traction equilibrium equations are collocated at the interface and outer surface nodes. Compared with the standard finite element method, no integrals are involved to form the coefficients of the system and a reduced and lumped mass matrix can be directly obtained from the density properties of the target problem. Since the mass term only exists at the internal nodes of elements, the dynamic coupling of final system equations of the structure can be reduced, which will greatly save the computational resources. Numerical examples about free and forced 2D and 3D dynamic problems are given to demonstrate the correctness and efficiency of the proposed method.

1. Introduction

The vibration and wave propagation are of great interest for all fields of science and engineering, which is governed by a set of second-order, coupled differential equations, with a proper set of initial and boundary conditions. Various numerical methods are available to solve the elastodynamic problems [1–8], which generally can be classified into two types: the weak-form techniques and strong-form techniques. Although the weak-form techniques, such as the finite element method (FEM) [9], isogeometric analysis method [4], boundary element method [10], finite volume method [11] have been widely used in many engineering problems, the strong-form techniques including the point collocation methods [12], conventional finite difference method [13] have also shown great vitality and bright prospects due to the fact that no variational principles or energy principles are required and no elemental integrals exist.

The collocation methods are types of numerical methods to approximate the solutions of boundary value problems based on the strong form of partial differential equations [5]. Tornabene et al. [14,15] proposed a strong formulation point collocation method which uses the hybrid scheme given by the FEM and differential quadrature method. The differential quadrature method is a part of more general family of the spectral collocation methods. Shu [16] proposed a generalized differential quadrature method which leads to a simpler and straightfor-

ward implementation of systems of partial differential equations. The method turned out to be useful and stable for studying structural components and the mechanics of composite structure, beams, plates and shells [17–18]. On the other hand, the collocation method was recently used within the framework of the isogeometric analysis, named as isogeometric collocation methods [19–21]. Researches indicated that the isogeometric collocation methods can not only preserve the advantages of isogeometric method in terms of geometrical flexibility and accuracy but also can minimize the computational cost. Moreover, in the literature some works about the collocation methods used strong form formulation based on other interesting techniques have also been reported, such as the modified finite particle method [22, 23], the Collocation-Galerkin method [5], and the superconvergent meshfree collocation method [24].

One of the important applications based on the strong form techniques is to solve the elastodynamics problems in the time and frequency domains. Tornabene et al. [14] proposed a local generalized differential quadrature method to solve the free vibration analysis of doubly-curved laminated composite shells and panels based on general higher-order theories. Fantuzzi [25] investigated the numerical stability and accuracy of strong form FEM related to elastostatic and elastodynamic problems. Viola et al. [2] investigated the dynamic behavior of moderately thick composite plates of arbitrary shape using the generalized differential quadrature method. The free vibration behavior of arbitrary shaped functionally graded plates was analyzed by the strong-

* Corresponding author.

E-mail address: xwgao@dlut.edu.cn (X.-W. Gao).

form method [26], and the result indicates that the method can provide stable and accurate solutions. Since the strong form technique does not require the derivation of the weak form of the governing equation like the FEM, it can greatly reduce formulation efforts in higher order approximation [27]. Thus, it is worth to develop strong-form techniques to solve vibration problems of 3D structures in real engineering applications.

In this work, the authors will focus on developing a new strong-form numerical element method to solve elastodynamics problems of solids. In literature, many investigators focus on new strong formulations of the governing equations aiming at solving more complicated structures with more accuracy. Wen and Li [28–29] proposed a finite block method, a type of strong-form algorithm based on the point collocation method, to solve heat conduction problem in the functionally graded media and anisotropic materials. And the method was further extended to solve 2D and 3D elasticity problems. Fantuzzi et al. [30] proposed a strong-form FEM for solving solid elastodynamic problems, which incorporates the mapping technique proper of FEM or isogeometric analysis method and the strong form collocation approach. Recently, the element differential method (EDM) as a new strong form technique, has been proposed by Gao et al. [31, 32] for solving general boundary value problems of the second order partial differential equations. The idea of FEM in the aspect of using isoparametric elements has been borrowed to obtain the global spatial derivatives, and the idea of collocation-like methods has been learned in the aspect of collocating equations at nodes. A set of analytical formulations of the spatial derivatives for 2D and 3D problems are derived explicitly and expressed through shape functions of elements, which can be used for the physical variables' differentiation of arbitrary systems. The method has been successfully used to solve general heat conduction and solid mechanics problems [31, 32]. The results indicate that EDM is easier to be coded than FEM and able to generate smaller system and more accurate results than finite block method and can obtain more stable solution than other collocation methods.

The objective of the present research is to extend the EDM to solve free and forced vibration problems of complicate structures. As pointed by Gao et al. [31, 32], one of the important features of the elements used in EDM is that an internal node should be placed inside the elements. Thus, the 2D 9-node quadrilateral and 3D 27-node hexahedral Lagrange isoparametric elements are utilized here to mesh the 2D and 3D structures, respectively. In EDM, there is no need to use mathematical or mechanical principles to set up the system equations. In contrast, the dynamic system equations can be generated directly by a new collocation method performed on the resulting isoparametric elements. In this method, the dynamic equilibrium equations are collocated only at the internal nodes of an element, and the traction equilibrium equations are collocated at the interface and outer surface nodes. It can be found that a lumped mass matrix which is similar to those used in standard FEM can be directly calculated and obtained in this collocation scheme. The diagonal form of the lumped mass matrix will show the superiority over the consistent mass matrix (compared with standard FEM) in data recording and algebraic equation solving, especially in the explicit dynamic analysis. Moreover, since the mass term is only placed on internal nodes, the basic substructuring idea is introduced to transform the system equations, which will lead to a reduced dynamic system equation that only contains the unknowns of internal nodes. At last, the free and forced vibration problems can be efficiently solved on the reduced dynamic system equation. Several numerical examples about free and forced 2D and 3D dynamic problems are given to demonstrate the correctness and efficiency of the proposed method.

The rest of the paper is organized as follows: first, the governing equations of dynamic problems for elastic materials are presented. The discrete method of the governing equation for dynamic problems using the EDM is derived in detail. The solution procedure of the free and forced vibration problems based on the obtained system equations is given in Section 4. Numerical examples are provided next, and finally conclusions are summarized.

2. Governing equation for dynamic linear elasticity

The differential equation for linear dynamic problems can be described by the following equilibrium equation

$$\frac{\partial \sigma_{ij}}{\partial x_j} + b_i - \rho \frac{\partial^2 u_i}{\partial t^2} - \mu \frac{\partial u_i}{\partial t} = 0 \quad x \in \Omega \quad (1)$$

where σ_{ij} is the stress tensor, b_i the body force, ρ the density of the structure, μ damping coefficients, Ω the computational domain, and the repeated index j stands for the summation.

The stress tensor σ_{ij} can be expressed in terms of the strain tensor

$$\sigma_{ij} = D_{ijkl}(x)\epsilon_{kl} \quad (2)$$

where, $D_{ijkl}(x)$ is the elastic constitutive tensor, which can vary with the coordinates. The strain tensor ϵ_{kl} can be written as

$$\epsilon_{kl} = \frac{1}{2} \left(\frac{\partial u_k}{\partial x_l} + \frac{\partial u_l}{\partial x_k} \right) \quad (3)$$

The boundary conditions (Traction t_i on the surface Γ_t and constraints on the surface Γ_u of the problem can be expressed as:

$$t_i = \sigma_{ij} n_j \quad (4a)$$

$$u_i(x) = \bar{u}_i(x) \quad (4b)$$

where the initial conditions can be written as

$$\begin{cases} u_i(x, 0) = u_i(x) \\ u_{i,t}(x, 0) = u_{i,t}(x) \end{cases} \quad (5)$$

On substituting Eq. (2) into Eq. (3), and the results into Eq. (1), the boundary value problem in the linear dynamic analysis can be described by the following second order partial differential equation:

$$D_{ijkl} \frac{\partial^2 u_k}{\partial x_j \partial x_l} + \frac{\partial(D_{ijkl})}{\partial x_j} \frac{\partial u_k}{\partial x_l} + b_i - \rho \frac{\partial^2 u_i}{\partial t^2} - \mu \frac{\partial u_i}{\partial t} = 0 \quad (6)$$

and the boundary conditions can be written as:

$$\begin{cases} u_i(x) = \bar{u}_i(x), & x \in \Gamma_u \\ t_i(x) = D_{ijkl}(x)n_j(x) \frac{\partial u_k(x)}{\partial x_l}, & x \in \Gamma_t \end{cases} \quad (7)$$

where Γ_u and Γ_t are the boundaries specified by the displacement \bar{u}_i and the traction \bar{t}_i , respectively, with $\Gamma_u \cup \Gamma_t = \Gamma$.

3. Discretizing governing equations with element differential method

This section formulates the EDM for dynamic problems. Similar as FEM, firstly the computation domain needs to be discretized into a series of elements, which contains an internal node. The differentiation of the shape functions of the elements can be derived directly used to characterize the geometry and physical variables in EDM [31]. And then, the governing equations of the dynamic problems, which are composed of first and second order partial derivatives equations, can be further expressed as derivative of the shape functions with respect to global coordinates. At last, a new type of collocation methods is proposed based on the analytical expression about the derivatives to establish the final system of equations. In this method, the equilibrium equations are collocated at nodes placed inside the elements, and the traction equilibrium equations are collocated at interface nodes between elements and outer surface nodes of the problem.

3.1. Shape functions for Lagrange isoparametric elements

In current research, the Lagrangian isoparametric elements are introduced to discretize the elastodynamic problems. As indicated in our previous work, an important feature of the elements used in EDM is that an internal node should be located inside the elements. Thus, for simplicity, those Lagrange isoparametric elements where a node located

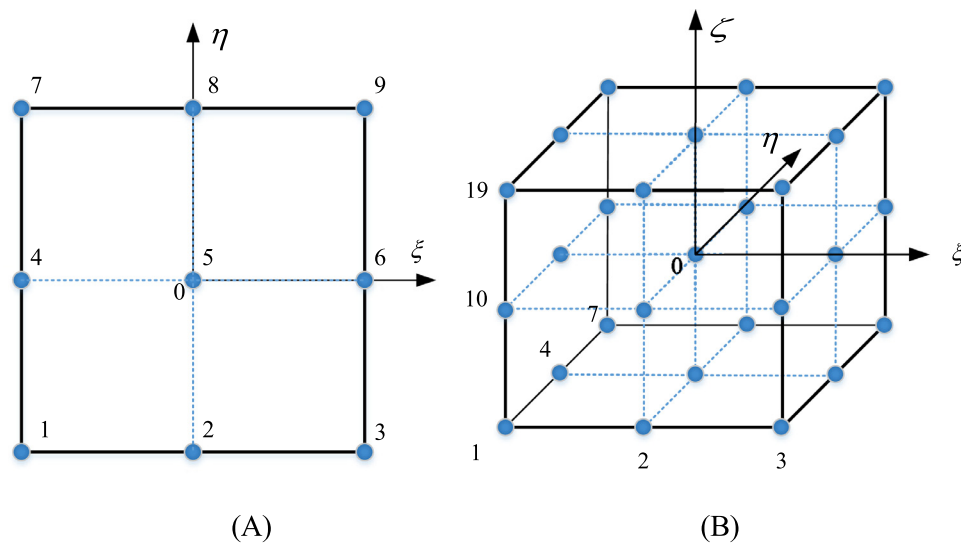


Fig. 1. Lagrange isoparametric elements: (A) 9-node 2D quadrilateral element, and (B) 27-node 3D brick element.

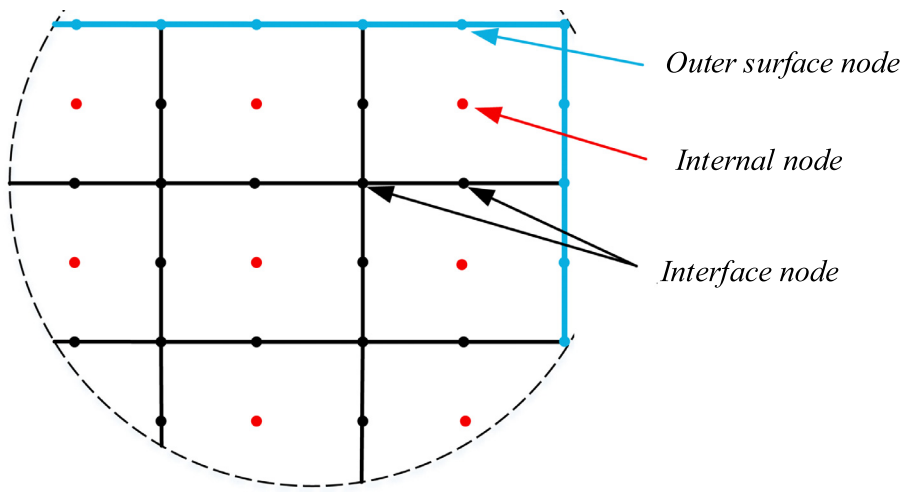


Fig. 2. Three types of nodes in the system equations: outer surface nodes, internal nodes and interface nodes.

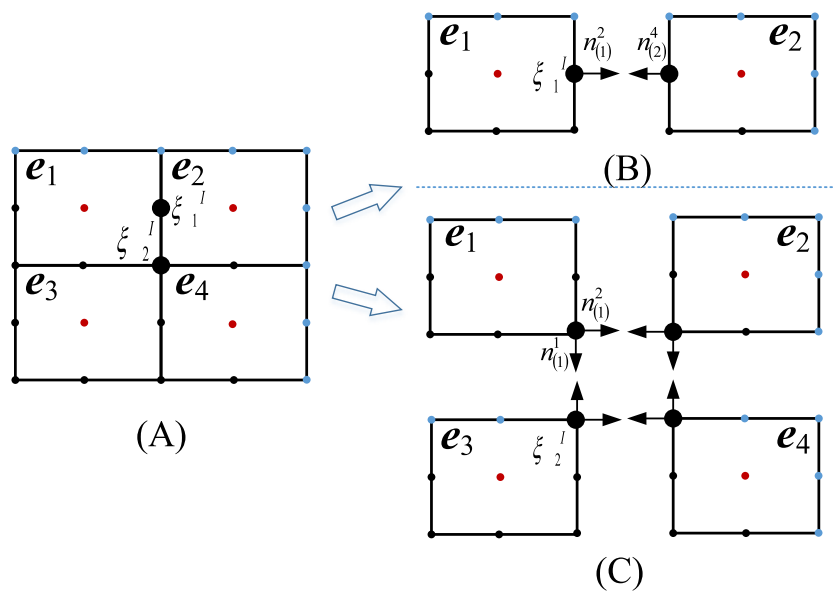


Fig. 3. Collocation technique for element interface nodes: (A) Structure meshed with Lagrangian elements; (B) interface node shared with 2 elements; (C) interface node shared with 4 elements.

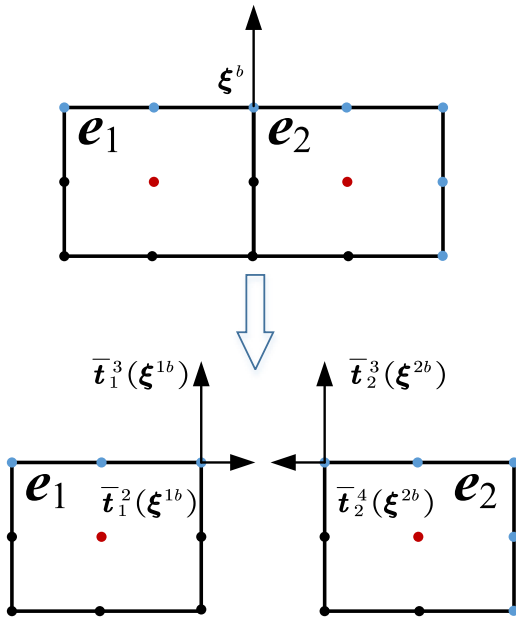


Fig. 4. Collocation technique for element interface nodes.

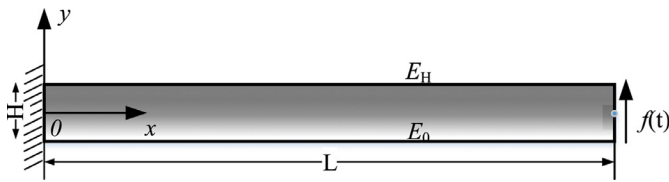


Fig. 5. Geometry of the 2D cantilever beam.

inside are utilized to mesh the 2D and 3D structures, such as the 9-node quadrilateral elements and 27-node hexahedral elements, as illustrated in Fig. 1.

The shape functions of the Lagrangian isoparametric elements and their partial derivatives are firstly briefly described here and more details can be found in our previous works [32]. For 1D isoparametric elements, the shape functions can be determined by the Lagrange interpolation formulation [9]:

$$L_I^m(\xi) = \prod_{i=1, i \neq I}^m \frac{\xi - \xi_i}{\xi_I - \xi_i} (I \sim m) \quad (8)$$

where ξ is the natural coordinate in the elements given by $-1 \leq \xi \leq 1$, ξ_i is the isoparametric coordinate of interpolation point, and m is the number of interpolation points. Using this form of interpolation, the

Lagrangian family of elements can be expressed as products of the one-dimensional functions. For example, the shape function for 2D elements can be given by

$$N_\alpha(\xi, \eta) = L_I^m(\xi) L_J^n(\eta) \quad (9)$$

and the shape function for 3D elements can be expressed as

$$N_\alpha(\xi, \eta, \zeta) = L_I^m(\xi) L_J^n(\eta) L_K^p(\zeta) \quad (10)$$

where the subscript α is determined by the permutation of the subscripts I , J , and K sequentially. The superscripts m , n , and p are the number of the interpolation points along ξ , η and ζ directions, respectively.

3.2. Expressing coordinates and physical variables in terms of element nodal values

The isoparametric formulation may be used for any problem in which the approximations are C^0 continuous. In an isoparametric formulation, a parent element is defined in terms of a set of natural coordinates. The shape functions defined above are constructed on a parent element and used to compute the coordinates and displacements with each elements using

$$x_i = N_\alpha(\xi)x_i^\alpha \quad (11a)$$

$$u_i = N_\alpha(\xi)u_i^\alpha \quad (11b)$$

where $\xi = (\xi, \eta, \zeta)$ are a set of natural coordinates, x_i^α and u_i^α are the nodal values of coordinates and displacements.

In problems using C^0 continuous it is necessary to construct the derivatives of variables with respect to the global coordinates. For an isoparametric formulation these derivatives are computed as derivatives of the shape functions with respect to global coordinates by

$$\frac{\partial u_k}{\partial x_i} = \frac{\partial N_\alpha}{\partial x_i} u_k^\alpha \quad (12a)$$

$$\frac{\partial^2 u_k}{\partial x_i \partial x_j} = \frac{\partial^2 N_\alpha}{\partial x_i \partial x_j} u_k^\alpha \quad (12b)$$

Based on the interpolation scheme, the governing equation Eq. (6) within an element can be expressed as follows:

$$\left[D_{ijkl}(\xi) \frac{\partial^2 N_\alpha(\xi)}{\partial x_l \partial x_j} + \frac{\partial N_\beta(\xi)}{\partial x_j} D_{ijkl}^\beta \frac{\partial N_\alpha(\xi)}{\partial x_l} \right] u_k^\alpha + b_i - \rho N_\alpha(\xi) \frac{\partial^2 u_i^\alpha}{\partial t^2} - \mu N_\alpha(\xi) \frac{\partial u_i^\alpha}{\partial t} = 0 \quad (13)$$

Fig. 6. Meshes of the 2D cantilever beam:
(a) 160 regular quadratic elements
(b) 346 irregular quadratic elements
(c) 640 regular quadratic elements.

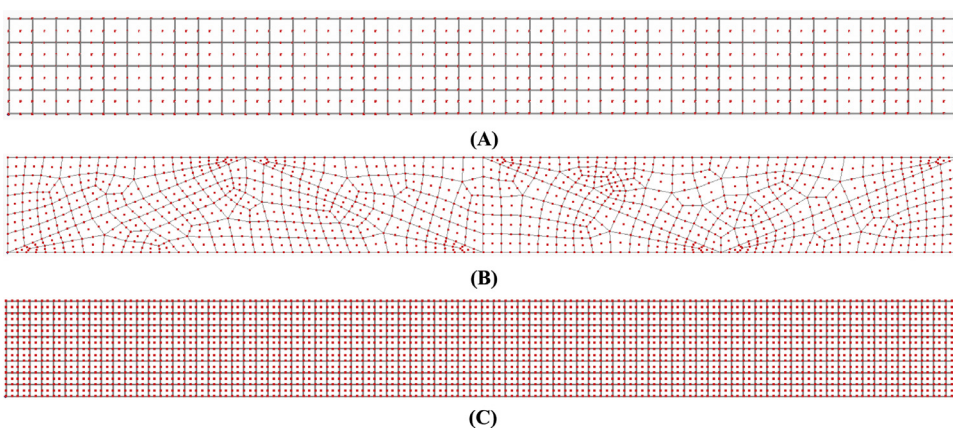


Table 1

Natural frequencies of the homogeneous beam calculated by EDM and FEM based on different mesh grids (rad/time).

Orders	EDM (160)	EDM (346)	EDM (640)	FEM (160)	FEM (640)	FEM (1E4)
1st	0.0536	0.0543	0.0539	0.0549	0.0542	0.0539
2nd	0.3210	0.3254	0.3223	0.3283	0.3241	0.3225
3rd	0.8424	0.8417	0.8418	0.8420	0.8417	0.8415
4th	0.8439	0.8505	0.8462	0.8611	0.8506	0.8465
5th	1.5306	1.5425	1.5326	1.5577	1.5397	1.5326
6th	2.3314	2.3484	2.3306	2.3653	2.3398	2.3296

Table 2

Natural frequencies for the FGM beam calculated by EDM and FEM based on different mesh grids (rad/time).

Orders	EDM (160)	EDM (346)	EDM (640)	FEM (160)	FEM (640)	FEM (1E4)
1st	0.0345	0.0348	0.0340	0.0338	0.0333	0.0331
2nd	0.2068	0.2050	0.2035	0.2023	0.1994	0.1983
3rd	0.5409	0.5355	0.5331	0.5290	0.5223	0.5197
4th	0.5642	0.5632	0.5635	0.5535	0.5526	0.5522
5th	0.9875	0.9804	0.9716	0.9645	0.9518	0.9468
6th	1.5011	1.4921	1.4764	1.4640	1.4458	1.4385

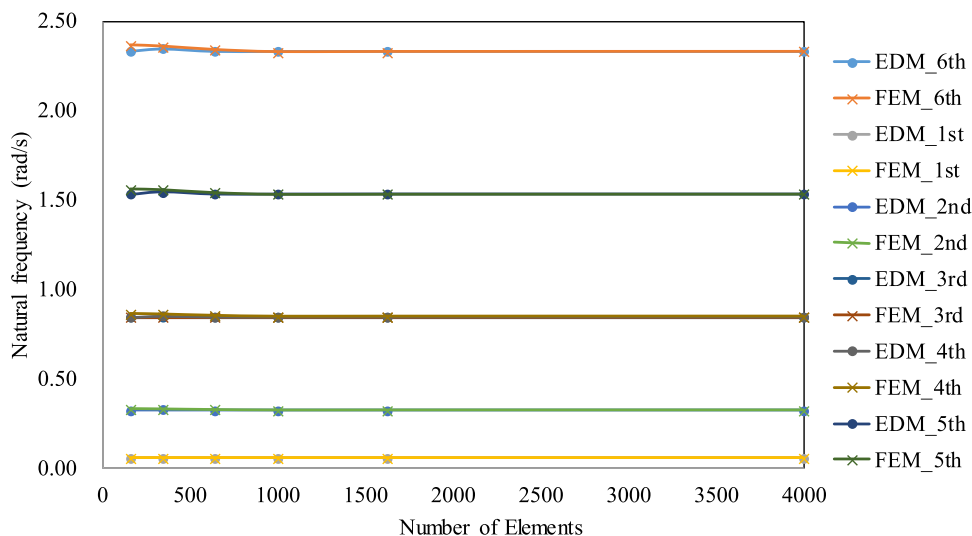


Fig. 7. Natural frequencies for the homogeneous beam calculated by EDM and FEM based on different mesh grids (rad/time).

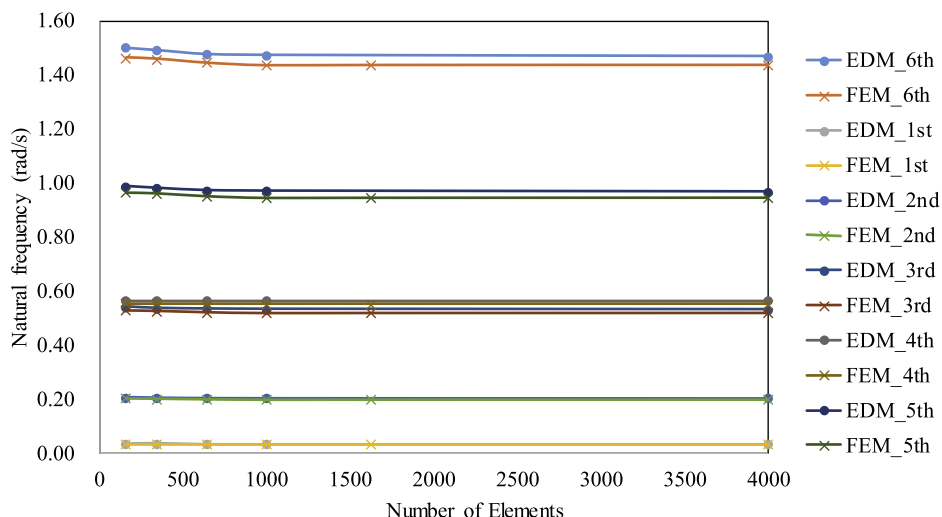
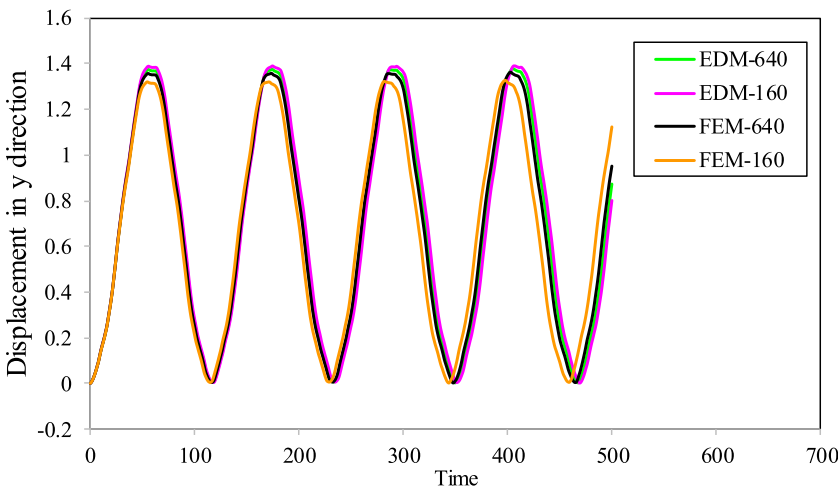
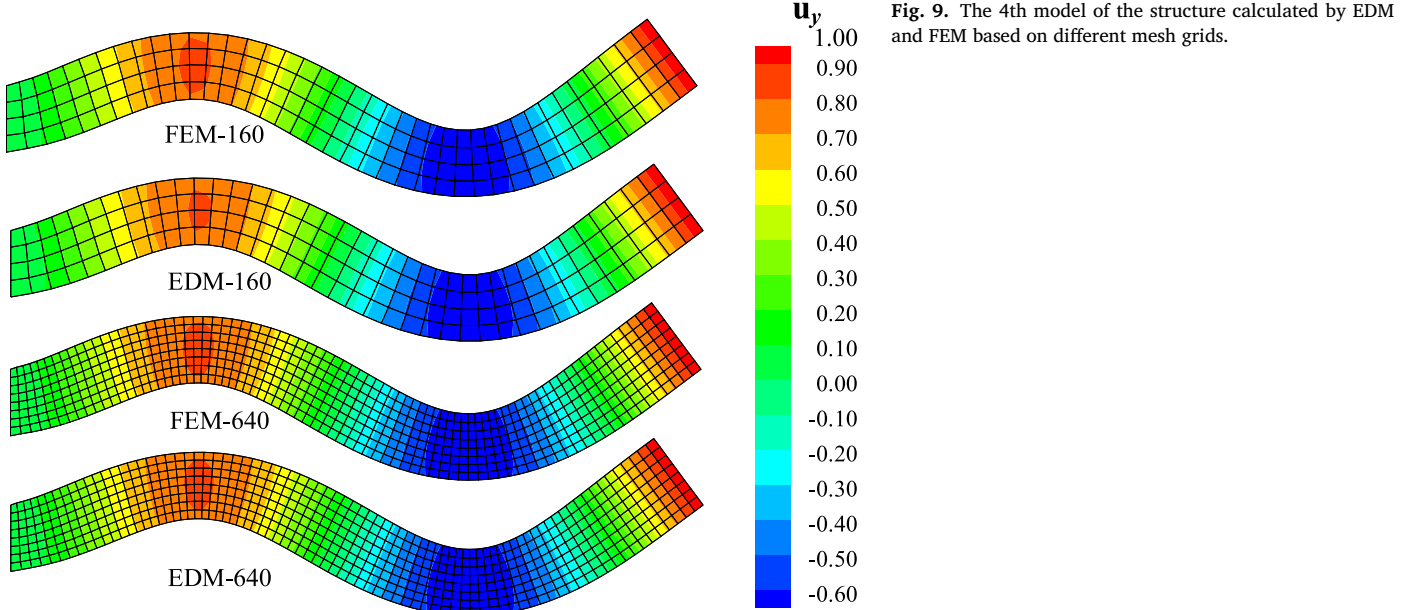


Fig. 8. Natural frequencies for the FGM beam calculated by EDM and FEM based on different mesh grids (rad/time).



3.3. Derivatives of elemental shape functions with respect to global coordinates

It can be observed from Eq. (13) that the key task to solve the dynamic problem is to establish an algorithm to compute the first and second order partial derivatives of the physical variables, i.e., the displacement, with respect to global spatial coordinates. In EDM, these partial derivatives are analytically derived based on the shape functions given above [32].

As indicated in Eqs. (9) and (10), the shape functions $N_\alpha(\xi)$ are the explicit functions of natural coordinates ξ , thus the first and second order partial derivatives in an isoparametric formulation can be computed using the chain rule given by

$$\frac{\partial N_\alpha}{\partial x_i} = \frac{\partial N_\alpha}{\partial \xi_k} \frac{\partial \xi_k}{\partial x_i} = [J]_{ik}^{-1} \frac{\partial N_\alpha}{\partial \xi_k} \quad (14)$$

$$\frac{\partial^2 N_\alpha}{\partial x_i \partial x_j} = \left[[J]_{ik}^{-1} \frac{\partial^2 N_\alpha}{\partial \xi_k \partial \xi_l} + \frac{\partial [J]_{ik}^{-1}}{\partial \xi_l} \frac{\partial N_\alpha}{\partial \xi_k} \right] \frac{\partial \xi_l}{\partial x_j} \quad (15)$$

where $[J] = [\partial x / \partial \xi]$ is the Jacobian matrix mapping from the global coordinate system x_i to the natural coordinate system ξ_k . The $\frac{\partial \xi_l}{\partial x_j}$, $[J]_{ik}^{-1}$

and $\frac{\partial [J]_{ik}^{-1}}{\partial \xi_l}$ in Eqs. (14) and (15) can be determined explicitly, which can

be found in the work [31]. As a consequence, the terms $\frac{\partial N_\alpha}{\partial \xi_k}$ and $\frac{\partial^2 N_\alpha}{\partial \xi_k \partial \xi_l}$ in Eqs. (14) and (15) can be explicitly obtained by directly differentiating Eq. (9) for 2D or Eq. (10) for 3D problems. Using the above analytical expressions, the first and second order spatial derivatives of the shape functions with respect to global coordinates can be calculated.

3.4. New collocation technique

In this section, the new collocation technique, which has been successfully applied to generate system equations of the static mechanical and heat conduction problems and provide very stable results [31, 32], is adopted to assemble the global algebraic system for the dynamic problems. Different from traditional collocation methods, the governing equations and the traction equilibrium equations are separately collocated with different rules here. Taking the two dimensional problems for an example (see Fig. 2), the nodes of the elements can be classified as outer surface nodes, internal nodes and the interface nodes. Thus, the governing equations of the problems are collocated only at the internal nodes, while the traction equilibrium equations are collocated at the interface and outer surfaces nodes. In what follows, the final system of equations for the dynamic problems established with the new collocation rules will be introduced in detail.

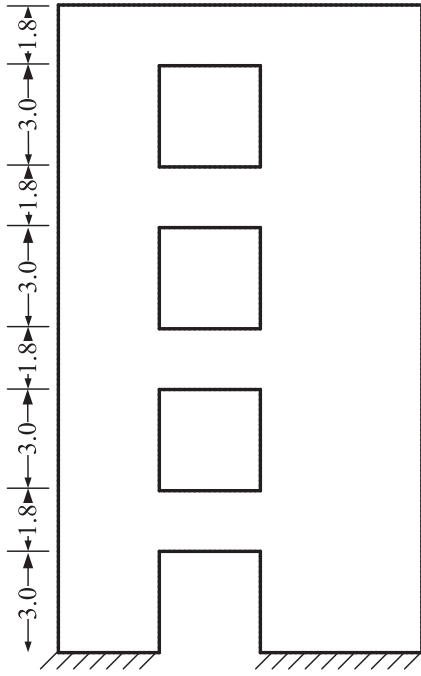


Fig. 11. A shear wall with four openings.

3.4.1. Collocation technique for internal nodes

The equation for internal nodes of elements can be collocated based on the equilibrium equations. As indicated in Fig. 2, the internal nodes refer to the nodes located within the elements, at which the governing equation Eq. (13) should be satisfied. The governing equation for the internal nodes can be rewritten as:

$$\left[D_{ijkl}(\xi) \frac{\partial^2 N_a(\xi)}{\partial x_i \partial x_j} + \frac{\partial N_\beta(\xi)}{\partial x_j} D_{ijkl}^\beta \frac{\partial N_a(\xi)}{\partial x_l} \right] u_k^\alpha + b_i - \rho \frac{\partial^2 u_i^I}{\partial t^2} - \mu \frac{\partial u_i^I}{\partial t} = 0 \quad (16)$$

where u_k^α indicates the node value of displacement in k direction at nodes α .

Thus, an algebraic system equation formulated based on Eq. (16) in terms of the element nodal values of displacement u_k^α and their first and second order derivatives with time (velocity $\frac{\partial u_i^I}{\partial t}$, acceleration $\frac{\partial^2 u_i^I}{\partial t^2}$) can be obtained. In this equation, the coefficients corresponding to acceleration and velocity can be considered as the mass and the damping matrix term of the elements. In other words, in EDM these mass and damping matrices can be directly captured from the density and damping coefficients. And they are only corresponding to internal nodes, respectively.

Thus, the consistent mass matrix obtained in this collocation scheme of the EDM is diagonal, which is similar as the lumped mass matrix used in standard FEM. As we know, it is very natural and convenient to use lumped mass matrix in FEM for the dynamic analysis [33]. The diagonal form of lumped mass matrix shows superiority over the consistent mass matrix in data recording and algebraic equation solving, especially in the explicit dynamic analysis. Its advantages will be shown in the examples mentioned in Section 5.

3.4.2. Collocation technique for element interface nodes

The equations for element interface nodes can be collocated based on traction equilibrium conditions. In EDM, these equilibrium conditions should be satisfied at the nodes located on the interface shared by a few elements. Thus, considering the traction equilibrium condition expressed in Eq. (7), the following equation can be set up by substituting Eq. (12) into Eq. (7):

$$\sum_{e=1}^{N^I} \sum_{s=1}^{S^{el}} D_{ijkl}(\xi^{el}) n_j^s(\xi^{el}) \frac{\partial N_a(\xi^{el})}{\partial x_l} u_k^\alpha = 0 \quad \xi^{el} \in \Gamma_I \quad (17)$$

where N^I is the number of elements including the interface node I , S^{el} the number of surfaces of element e associated with the interface node I . ξ^{el} the natural coordinate of element e at the interface node I . The n_j^s is the outward normal to element surface s . And Γ_I denotes the interface between elements. As indicated in Fig. 3A, here we still take the two dimensional problems for an example. Generally, two types of element interface nodes can be found in a structure meshed with higher order quadrilateral elements. In the first type the interface node I is shared with 2 elements with 2 surfaces (see Fig. 3B), thus N^I is set to 2 and S^{el} is set to 1. In the second type, the interface node I is shared with 4 elements with 8 element surfaces, N^I is equal to 4 and S^{el} is set to 2 for each element e (see Fig. 3C).

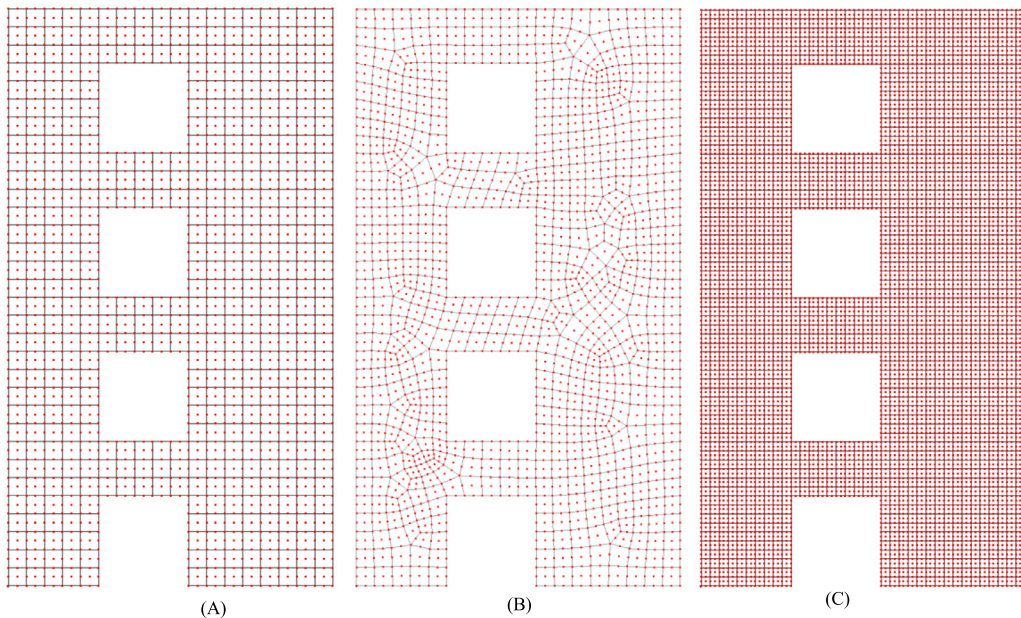


Fig. 12. Meshes of the shear wall: (a) 476 regular elements; (b) 562 irregular elements; (c) 1904 regular elements.

Table 3
Comparison of the natural frequencies (rad/s) of the shear wall.

Orders	EDM(476)	EDM (562)	FEM (476)	MLPG method [36]	Brebbia et al. [35]	FEM (7616)
1st	1.9687	1.9917	2.0732	2.069	2.079	2.0058
2nd	6.8736	6.9322	7.0956	7.153	7.181	6.9415
3rd	7.5850	7.5504	7.6253	7.742	7.644	7.5986
4th	11.239	11.354	11.938	12.163	11.833	11.435
5th	14.800	14.848	15.341	15.587	15.947	14.945
6th	17.892	17.862	18.345	18.731	18.947	18.053

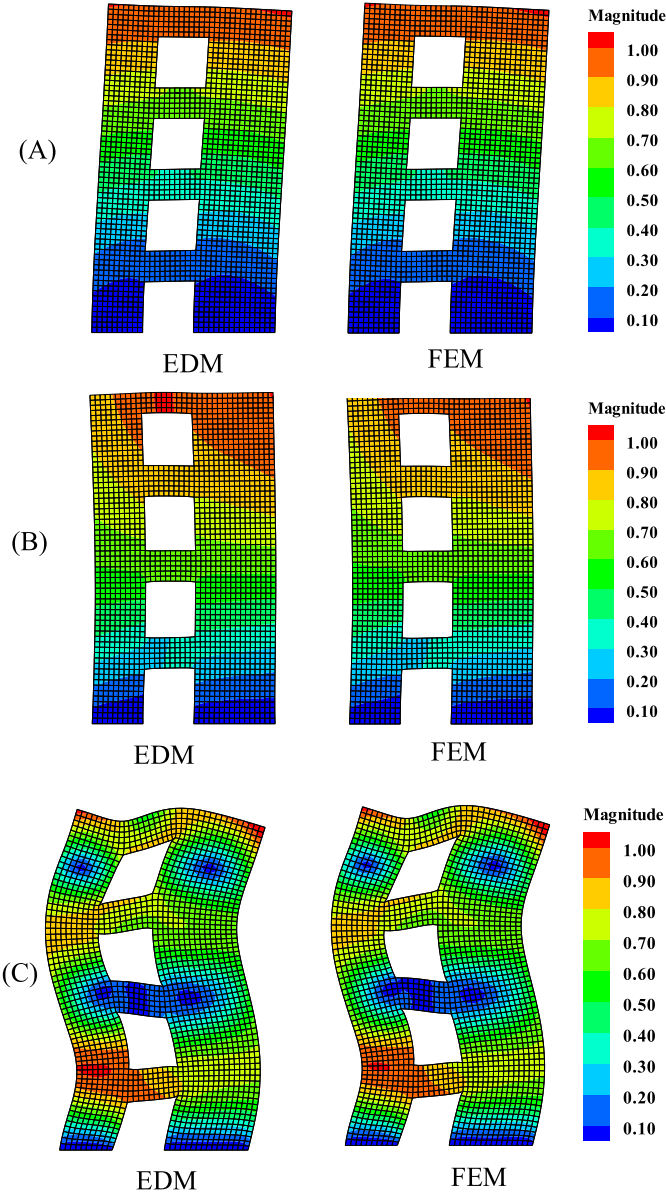


Fig. 13. Modes of the shear wall calculated by the EDM and FEM based on 1904 elements (A): 1st mode; (B) 2nd mode; (C) 3rd mode.

3.4.3. Collocation technique for outer boundary nodes

The equations for outer boundary nodes can also be collocated based on traction equilibrium conditions. The traction equilibrium conditions can be used for the nodes located on the outer boundaries of the problem.

$$\sum_{e=1}^{N^b} \sum_{s=1}^{S^{eb}} t_i^s(\xi^{eb}) = \sum_{e=1}^{N^b} \sum_{s=1}^{S^{eo}} \bar{t}_i^s(\xi^{eb}) \quad \xi^{eb} \in \Gamma_b \quad (18)$$

where N^b is the number of element including the boundary node b , S^{eb} and S^{eo} are the total number of interfaces and outer surfaces associated with the boundary node b , respectively. And \bar{t}_i is the specified external traction value. Thus, substituting Eq. (12) into Eq. (7), the traction equilibrium conditions for the boundary nodes can be expressed as

$$\sum_{e=1}^{N^b} \sum_{s=1}^{S^{eb}} D_{ijkl}(\xi^{eb}) n_j^s(\xi^{eb}) \frac{\partial N_a(\xi^{eb})}{\partial x_l} u_k^a = \sum_{e=1}^{N^b} \sum_{s=1}^{S^{eo}} \bar{t}_i^s(\xi^{eb}) \quad \xi^{eb} \in \Gamma_b \quad (19)$$

For instance, the boundary node b shared by 2 elements e_1 and e_2 , as indicated in Fig. 4. The external tractions $\bar{t}_1^3(\xi^{1b})$ and $\bar{t}_2^3(\xi^{2b})$ act on the third surfaces of the e_1 and e_2 , respectively. At the same time, the tractions $\bar{t}_1^2(\xi^{1b})$ and $\bar{t}_2^4(\xi^{2b})$ are applied on the second interface of e_1 and fourth interface of e_2 , respectively. In this case, $\bar{t}_1^2(\xi^{1b}) + \bar{t}_2^4(\xi^{2b}) = 0$ and only the tractions $\bar{t}_1^3(\xi^{1b})$ and $\bar{t}_2^3(\xi^{2b})$ need to be considered in Eq. (19).

3.4.4. Final equations for the dynamic problems

The final equations for the dynamic problems can be generated, once the special collocation method is performed on each nodes of the structures meshed with Lagrange isoparametric elements. First, equations involving nodal displacement values, velocity and acceleration can be generated by collocating Eq. (16) at all internal nodes and Eq. (17) at all interface nodes. At the same time, equations involving nodal displacement values and tractions can be generated by collocating Eq. (19) at all outer boundary nodes. Finally, these equations can be grouped together by defining global nodal vectors of displacement, velocity, acceleration and tractions, which are similar as those for the standard FEM.

The assembled final equations in EDM for the vibration problem can be written as (expressed in matrix form):

$$\dot{\mathbf{m}}\ddot{\mathbf{u}} + \dot{\mathbf{\mu}}\dot{\mathbf{u}} + \mathbf{K}\mathbf{u} = \mathbf{F} \quad (20)$$

where a dot over a variable denotes a time derivatives, \mathbf{m} the mass matrix, $\mathbf{\mu}$ the damping matrix, \mathbf{K} the stiffness matrix and \mathbf{F} the force vector. According to the rule of the collocation method mentioned above, the mass (density) and the damping terms are only corresponding to degrees of freedom of the internal nodes of each element. Thus the final equations (Eq. 20) can be rewritten as

$$\begin{bmatrix} \mathbf{0} & \mathbf{m}_{II} \end{bmatrix} \begin{bmatrix} \ddot{\mathbf{u}}_B \\ \ddot{\mathbf{u}}_I \end{bmatrix} + \begin{bmatrix} \mathbf{0} & \mathbf{\mu}_{II} \end{bmatrix} \begin{bmatrix} \dot{\mathbf{u}}_B \\ \dot{\mathbf{u}}_I \end{bmatrix} + \begin{bmatrix} \mathbf{K}_{BB} & \mathbf{K}_{BI} \\ \mathbf{K}_{IB} & \mathbf{K}_{II} \end{bmatrix} \begin{bmatrix} \mathbf{u}_B \\ \mathbf{u}_I \end{bmatrix} = \begin{bmatrix} \mathbf{F}_B \\ \mathbf{F}_I \end{bmatrix} \quad (21)$$

where \mathbf{u}_B and \mathbf{u}_I denotes the displacement matrix of nodes distributed at the boundary and inside of the elements, respectively. \mathbf{K}_{BB} , \mathbf{K}_{BI} , \mathbf{K}_{IB} and \mathbf{K}_{II} are substructures of element matrix \mathbf{K} . The vectors \mathbf{F}_B and \mathbf{F}_I are the nodal forces corresponding to boundary and internal nodes, respectively. The nonzero term of the mass and damping matrix can be written as

$$\mathbf{m}_{II} = \begin{bmatrix} -\rho & & & \\ & -\rho & & \\ & & \ddots & \\ & & & -\rho \end{bmatrix}, \quad \mathbf{\mu}_{II} = \begin{bmatrix} -u & & & \\ & -\mu & & \\ & & \ddots & \\ & & & -\mu \end{bmatrix} \quad (22)$$

4. Solution scheme to the dynamic system

The free (eigenvalue value problems) and forced vibrations of the structures can be solved based on the final equation of the dynamic

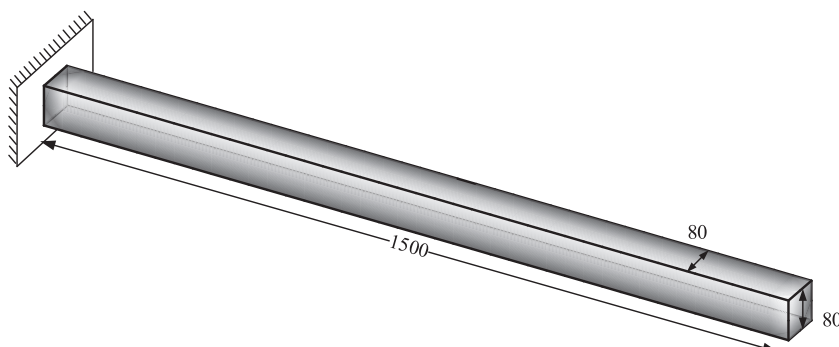


Fig. 14. Geometry of the 3D cantilever beam.

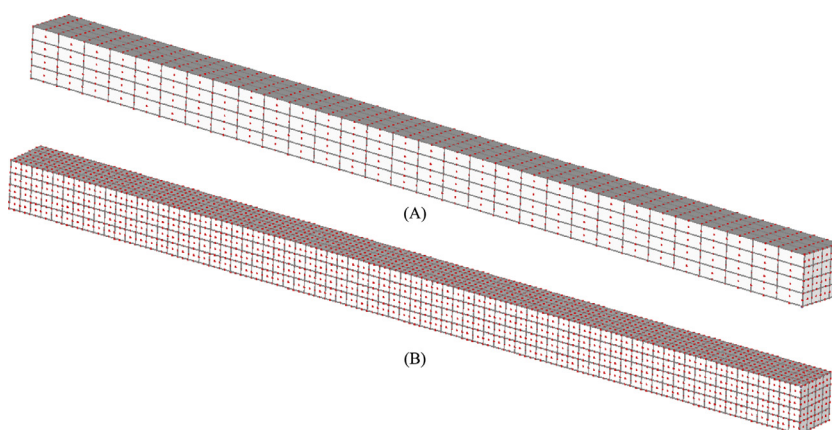


Fig. 15. Meshes of the 3D beam structure: (A) 480 elements; (B) 1200 elements.

Table 4
Comparison of the first 6 natural frequency calculated by EDM and FEM (rad/time).

Orders	EDM (480)	EDM (1200)	FEM (480)	FEM (1200)	FEM (18,800)
1st	6.3572	5.8298	6.0979	5.9696	5.8723
2nd	39.381	36.083	37.706	36.249	36.331
3rd	95.826	95.652	95.130	95.116	98.341
4th	108.37	99.123	103.47	101.35	99.738
5th	170.99	170.75	170.71	170.71	170.65
6th	207.46	189.21	197.25	193.24	190.21

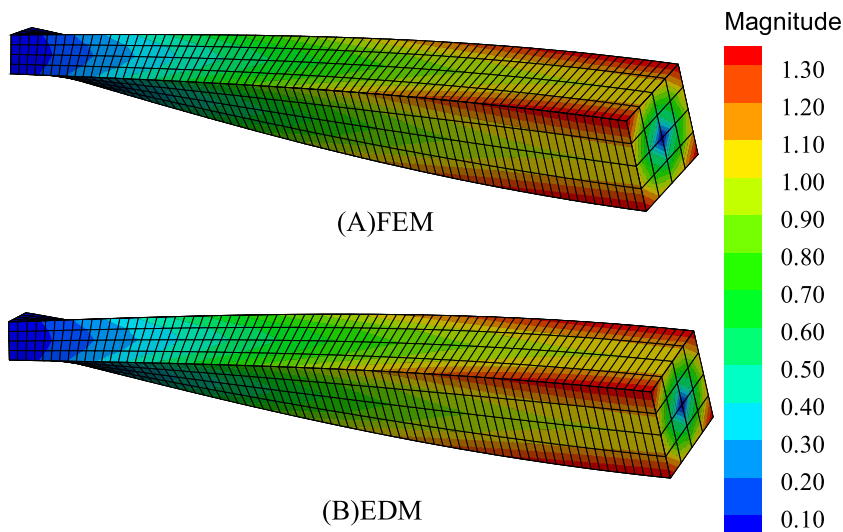


Fig. 16. Comparison of the torsional modes calculated by (A) FEM and (B) EDM based on 1200 elements.

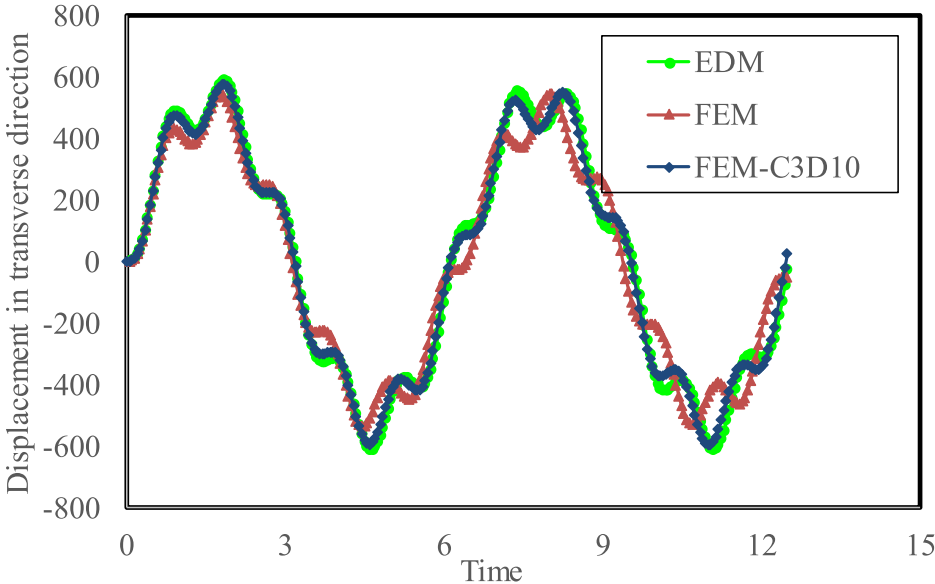


Fig. 17. Transient responses of the 3D cantilever beam subjected to harmonic shear force.

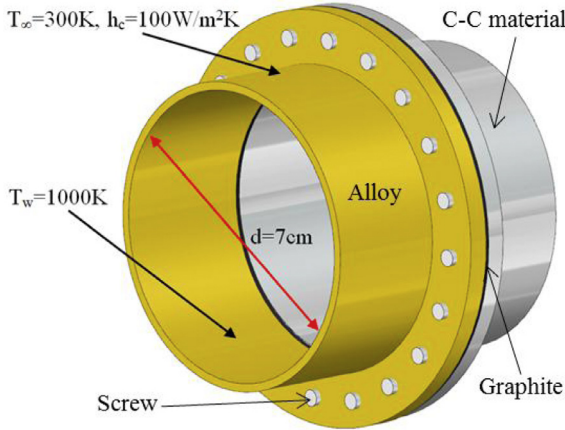


Fig. 18. A connector of a circular combustor of an aeroengine [30].

problems. It can be found that Eq. (21) is not a standard dynamic equation of structure motions, where the mass and damping terms in the equations are nonzero for only those nodes within the element. In other word, in order to utilize the traditional algorithms to solve free/forced vibration problems, one needs to perform some transformation on the final system equations.

4.1. Transformation of final equations for motions

In this section the basic substructuring idea is introduced to transform the equations obtained above. The main idea is to eliminate all degree of freedom of the boundary nodes of elements. For the sake of simplicity, the damping terms in the system are neglected in Eq. (22), and only the linear dynamic problem is considered here. The resulting equation of motions can be rewritten as:

$$\begin{bmatrix} \mathbf{0} & \mathbf{m}_{II} \end{bmatrix} \begin{bmatrix} \ddot{\mathbf{u}}_B \\ \ddot{\mathbf{u}}_I \end{bmatrix} + \begin{bmatrix} \mathbf{K}_{BB} & \mathbf{K}_{BI} \\ \mathbf{K}_{IB} & \mathbf{K}_{II} \end{bmatrix} \begin{bmatrix} \mathbf{u}_B \\ \mathbf{u}_I \end{bmatrix} = \begin{bmatrix} \mathbf{F}_B \\ \mathbf{F}_I \end{bmatrix} \quad (23)$$

Thus, the equation above can be expressed as two equations:

$$\mathbf{K}_{BB}\mathbf{u}_B + \mathbf{K}_{BI}\mathbf{u}_I = \mathbf{F}_B \quad (24a)$$

$$\mathbf{m}_{II}\ddot{\mathbf{u}}_I + \mathbf{K}_{IB}\mathbf{u}_B + \mathbf{K}_{II}\mathbf{u}_I = \mathbf{F}_I \quad (24b)$$

Table 5
Mechanical and thermal material properties.

Materials	Young's modulus, E (GPa)	Poisson ratio, ν	Density (Kg/m ³)
Alloy	179.5	0.327	2820.0
C-C material	90.0	0.2	2820.0
graphite	1.38	0.05	2820.0

According to Eq. (24a), the displacements of the boundary nodes can be calculated by

$$\mathbf{u}_B = \mathbf{K}_{BB}^{-1}(\mathbf{F}_B - \mathbf{K}_{BI}\mathbf{u}_I) \quad (25)$$

Then integrating Eq. (25) into Eq. (24b), one gets the equation

$$\mathbf{m}_{II}\ddot{\mathbf{u}}_I + (\mathbf{K}_{II} - \mathbf{K}_{IB}\mathbf{K}_{BB}^{-1}\mathbf{K}_{BI})\mathbf{u}_I = \mathbf{F}_I - \mathbf{K}_{IB}\mathbf{K}_{BB}^{-1}\mathbf{F}_B \quad (25)$$

Thus Eq. (25) leads to a standard dynamic equation of motions:

$$\mathbf{M}^*\ddot{\mathbf{u}}_I + \mathbf{K}^*\mathbf{u}_I = \mathbf{F}^* \quad (26)$$

where

$$\mathbf{M}^* = \mathbf{m}_{II} \quad (27a)$$

$$\mathbf{K}^* = \mathbf{K}_{II} - \mathbf{K}_{IB}\mathbf{K}_{BB}^{-1}\mathbf{K}_{BI} \quad (27b)$$

$$\mathbf{F}^* = \mathbf{F}_I - \mathbf{K}_{IB}\mathbf{K}_{BB}^{-1}\mathbf{F}_B \quad (27c)$$

It can be found that under the transformation the dynamic equation Eq. (26) is a standard dynamic equation of motions, where the response of the system can be defined by the stiffness and mass of the retained degrees of freedom denoted by the vector \mathbf{u}_I . The free or forced vibration problems based on dynamic equations Eq. (26) can be solved by the many existing methods [33].

4.2. Solution of free vibration problems

Based on the reduced dynamic equation of motion, we can easily obtain the eigenvalue equations to solve free vibration problems, which can be expressed as

$$\mathbf{K}^* \boldsymbol{\phi}_I = \omega^2 \mathbf{M}^* \boldsymbol{\phi}_I \quad (28)$$

where ω is the natural frequency of the whole structure, $\boldsymbol{\phi}_I$ the natural modal matrix corresponding to the retained degree of freedom of the inner nodes.

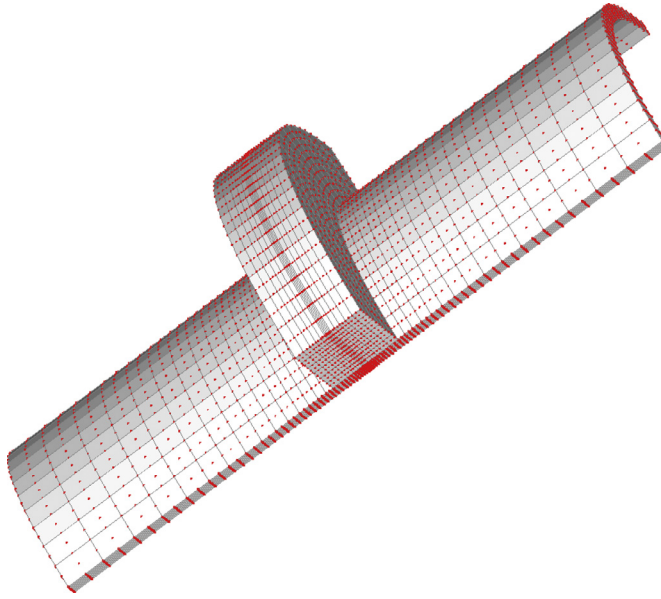


Fig. 19. The connector is discretized into 5400 27-node brick elements.

The eigenvalue equations Eq. (28) can be solved by many methods for the standard dynamic problems [32]. Once the natural frequency and the natural mode are calculated, the mode matrix of the boundary nodes can be calculated by

$$\Phi_B = -\mathbf{K}_{BB}^{-1} \mathbf{K}_{BI} \Phi_I \quad (29)$$

Therefore, the whole nature modal matrix of the structure can be written as

$$\Phi = \begin{bmatrix} \Phi_B \\ \Phi_I \end{bmatrix} \quad (30)$$

4.3. Solution of the dynamic response problems

The forced vibration of the dynamic problems can be solved by the reduced dynamic equations of motions (Eq. 26). Several methods are available to solve such equation in reference [34]. In current research, one of the well-known methods, Newmark time integration, is adopted to solve the problems [34]. The basic steps to solve the problem can be introduced as follows:

Given values of boundary and initial conditions (\mathbf{u}_I and $\dot{\mathbf{u}}_I$) at some time t , the values at time $t + \Delta t$ can be determined by using the governing equations of motion (Eq. 26). The Newmark time integration scheme is presented here.

Given \mathbf{K}^* , \mathbf{M}^* , \mathbf{F}^* , $\mathbf{u}_I(0)$, and $\dot{\mathbf{u}}_I(0)$:

Step 1: At $t = 0$, compute

$$\ddot{\mathbf{u}}_I(0) = \mathbf{M}^{*-1} [-\mathbf{K}^* \mathbf{u}_I(0) + \mathbf{F}^*(0)] \quad (31)$$

Step2: Then for successive time steps, solve the following equations for $\ddot{\mathbf{u}}_I(t + \Delta t)$

$$\begin{aligned} \mathbf{M}^* \ddot{\mathbf{u}}_I(t + \Delta t) + \frac{\beta_2 \Delta t^2}{2} \mathbf{K}^* \ddot{\mathbf{u}}_I(t + \Delta t) \\ = -\mathbf{K}^* \left[\mathbf{u}_I(t) + \Delta t \dot{\mathbf{u}}_I(t) + \frac{\Delta t^2}{2} (1 - \beta_2) \ddot{\mathbf{u}}_I(t) \right] + \mathbf{F}^*(t + \Delta t) \end{aligned} \quad (32)$$

Step3: Then compute $\mathbf{u}_I(t + \Delta t)$ and $\dot{\mathbf{u}}_I(t + \Delta t)$

$$\mathbf{u}_I(t + \Delta t) \approx \mathbf{u}_I(t) + \Delta t \dot{\mathbf{u}}_I(t) + \frac{\Delta t^2}{2} [(1 - \beta_2) \ddot{\mathbf{u}}_I(t) + \beta_2 \ddot{\mathbf{u}}_I(t + \Delta t)] \quad (33a)$$

$$\dot{\mathbf{u}}_I(t + \Delta t) \approx \dot{\mathbf{u}}_I(t) + \Delta t [(1 - \beta_1) \ddot{\mathbf{u}}_I(t) + \beta_1 \ddot{\mathbf{u}}_I(t + \Delta t)] \quad (33b)$$

Table 6

Comparison of the first 4 natural frequencies of the combustors calculated by the EDM and ABAQUS (rad/time).

Orders	EDM (ω_E)	ABAQUS(ω_A)	Errors($ \frac{\omega_E - \omega_A}{\omega_A} \times 100\%$)
1st	13037.6	14822.0	12%
2nd	16436.8	16600.2	1.0%
3rd	33809.8	36034.1	6.2%
4th	34507.3	36417.3	5.3%
5th	33156.4	36348.2	8.8%
6th	48493.6	46904.0	3.4%

where β_1 and β_2 are two adjustable parameters that determine the nature of the time integration scheme [34].

Step4: The displacement for other nodes

$$\mathbf{u}_B(t + \Delta t) = \mathbf{K}_{BB}^{-1} (\mathbf{F}_B - \mathbf{K}_{BI} \ddot{\mathbf{u}}_I(t + \Delta t)) \quad (34)$$

5. Numerical examples

To verify the correctness and demonstrate the potential of the proposed method, four numerical examples are given in this section. In the first and second examples, the two dimensional problems about a cantilever beam and four opening shear wall are analyzed, respectively. In the third example, the free and forced vibration problems of a three dimensional cantilever beam are investigated. And then the EDM is utilized to solve the free vibration response of a practical engineering structure, the connector of a circular combustor of an aero-engine. In above examples, the results calculated by EDM are compared with those calculated by FEM on fine scale grids or the values given by other methods in literatures to validate the correctness.

5.1. Two-dimensional cantilever beam

In this example, a cantilever beam is studied as shown in Fig. 5, with length $L = 10.0$, height $H = 1.0$, Poisson's ratio $\nu = 0.3$, mass density $\rho = 1.0$. A plane strain state is assumed. For the Young's modulus, two different cases are considered.

Case 1: Homogeneous beam: Young's modulus $E = 26.0$

Case 2: Materials gradation in y direction: $E = E(y) = E_0 e^{\alpha(y+H/2)}$

the gradient parameters α is determined by $\alpha = \frac{1}{H} \ln(\frac{E_H}{E_0})$, where $E_H/E_0 = 5.0$, $E_0 = 10.0$ is used in the calculation.

As illustrated in Fig. 6, several kinds of meshes including the regular elements (160, 640, 1625 and 4000 elements) and irregular elements (346 elements) are used in the analysis of the homogenous and functional grade material beams by EDM and FEM. Moreover, the results obtained by FEM on the fine mesh (1E4 elements), which is fine enough to obtain a converged result in the numerical analysis, are used as the reference results to examine the accuracy of numerical results.

First, the accuracy of the EDM in the calculation of eigenvalue problems is validated. Tables 1 and 2 listing the first six frequencies show a comparison of the natural frequencies for different meshes calculated by EDM and FEM methods. At the same time, the convergence rates of the natural frequencies of the two types of beams calculated by EDM and FEM are illustrated in Figs. 7 and 8, respectively. It can be found that the frequencies calculated by the EDM agree well with those calculated by FEM. Furthermore, the results calculated by EDM can have the same convergence rate and stable as those calculated by FEM. Fig. 9 plots the 4th mode of the structure calculated by the two methods based on the two types of mesh grids (160 and 640 elements). It can be observed the modes agree with each other which further indicate the accuracy of the proposed method.

Second, the forced vibration of the cantilever beam is analyzed. As indicated in Fig. 5, a transient load $f(t) = 0.005$, acts on the right end of the beam. Both EDM and FEM are utilized to compute the transient

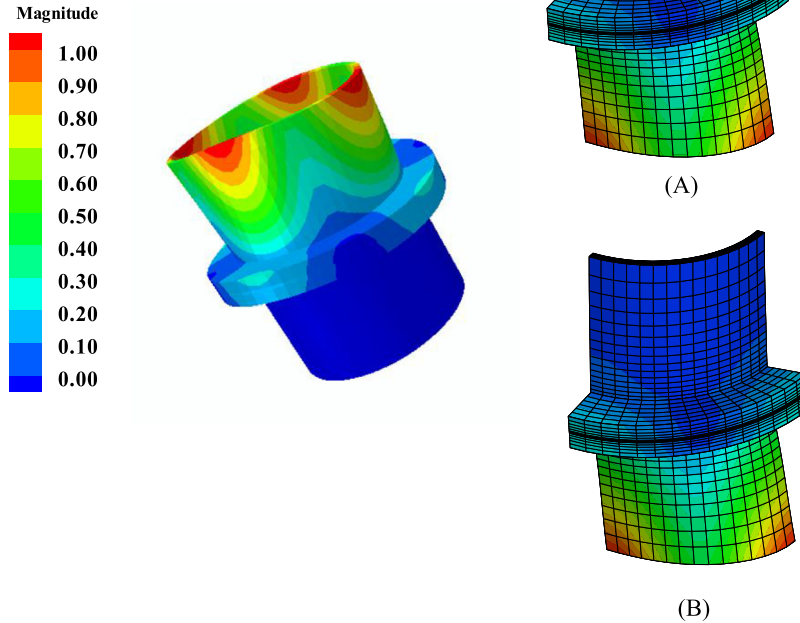


Fig. 20. First natural mode calculated by (A) EDM and (B) ABAQUS.

response of the structure. The implicit forced vibration solver Newmark method is used for both EDM and FEM. The parameters of Newmark method $\beta_1=0.25$, $\beta_2=0.5$. The time step $\Delta t=0.1$ is set for time integration, while the total computational time is set to 500.

The displacements in y direction of the node at the center of the right end are plotted in Fig. 10. It can be found that the results calculated by the EDM and FEM on different mesh grids agree well with each other, which further indicates the accuracy of the EDM to solve the forced vibration problems.

5.2. Free vibration of a shear wall

In this example, a shear wall with four openings is analyzed as illustrated in Fig. 11. The problem has been widely studied and solved in literatures using different methods, such as BEM, MLPG, and SFEM [35–37]. The bottom edge of the wall is fully clamped. The Young's modulus of the structure is $E=1.0E4$, Poisson's ratio is $\nu=0.2$, mass density $\rho=1.0$ and the plane stress state is considered here. The shear wall is meshed with 9-node quadrilateral element with 476, 1904 regular elements and 562 irregular elements, respectively, as shown in Fig. 12. The first six natural frequencies calculated by EDM and standard FEM as well as other results listing in literatures [37] which are based on the similar meshes are listed in Table 3. And the results calculated by FEM on mesh grids with 7616 elements, which is fine enough to obtain converged results, are used as the reference results. It is evident that the results calculated by the EDM agree well with those reference results obtained by the standard FEM at the same mesh grid. The first 6th mode shapes of the shear wall obtained by the EDM based on the mesh grid with 1904 elements are shown in Fig. 13.

5.3. Three-dimensional beam structure

In this example, a 3D cantilever beam is studied with dimension $80 \times 80 \times 1500$ mm, as illustrated in Fig. 14. Young' modulus $E=209$ GPa, Poisson's ratio $\nu=0.269$, and mass density

$\rho=7.89 \times 10^{-6}$ kg/mm³ are considered in this problem. The beam structure is meshed with 27-node hexahedral elements, and the two types of mesh grids (480 and 1200 elements) can be found in Fig. 15.

The free vibration problems are firstly analyzed by using the EDM and standard FEM. The reference solutions of free vibration of the beam are calculated by the fine scale meshes with 18,800 elements. Natural frequencies of the first 6 modes calculated from EDM and standard FEM are listed in Table 4. And the 5th order natural mode (free vibration of torsional system) of the beam is plotted in Fig. 16. Again the results calculated by EDM agree well with those reference results.

Second, the forced vibration of the cantilever beam is analyzed. A harmonic shear force $f(t)=50\sin(t)$ is loaded at the right end of the beam structure. The parameters of Newmark method is $\beta_1=0.25$ and $\beta_2=0.5$. The time step $\Delta t=0.05$ s is set for time integration, while the total computational time is set to 12.5 s.

The EDM and the FEM with the same number of elements (1200) are selected to solve this problem. The reference results are calculated by the commercial software ABAQUS on the same number of mesh grids, of which the selective reduce integration technique is used to obtain more accurate results. The dynamic responses of the cantilever beam are plotted in Fig. 17, from which we can observe that the amplitude of the EDM is closer to that of the reference solution. These results demonstrate that EDM can obtain much more accurate results than the standard FEM without any special techniques for forced vibration analyses.

5.4. Free vibration of the connector of a circular combustor

The last example is of the free vibration analysis of the connector of a circular combustor of an aeroengine, which is aimed to show the application potential of EDM to solve practical engineering problem. As illustrated in Fig. 18, three types of materials (Alloy, Graphite and C-C material) are used in these structures, of which the material properties are listed in Table 5 in detail [30]. The inner diameter of the combustor is 7 cm and the thickness of the combustor wall is 0.45 cm.

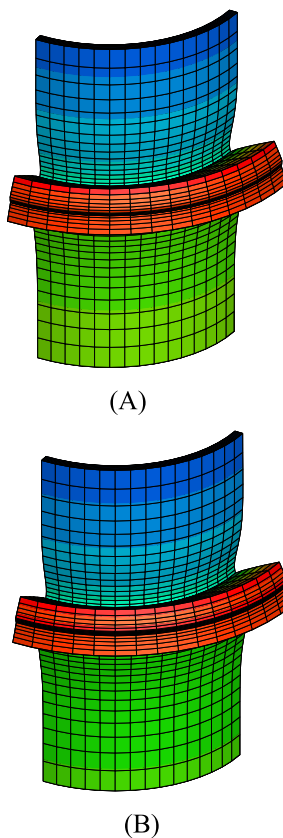
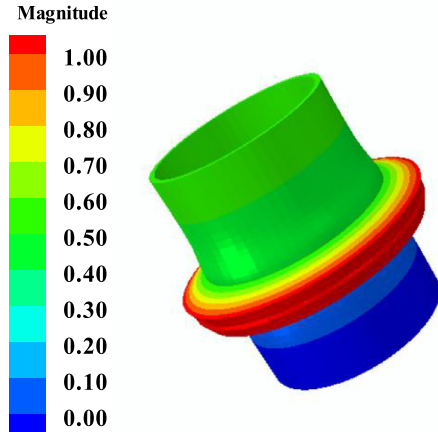


Fig. 21. Third natural mode calculated by (A) EDM and (B) ABAQUS.

The numerical model is constructed for a quarter of the combustor, as displaced in Fig. 19. The whole connector is discretized into 5400 27-node brick elements. For comparison, the problem is also computed using the standard FEM software ABAQUS based on the same number of meshes. The results of the first 4 natural frequencies are listed in Table 6. It can be see that the results of EDM have a good agreement with those obtained from the FEM software ABAQUS based on C3D8 elements. Moreover, the first and third order mode shapes of the combustor are plotted in Figs. 20 and 21 respectively. It can be observed that the EDM can accurately capture the mode shapes of the structure.

6. Conclusions

This paper highlights the potential of the numerical approach EDM for the free and forced vibration analyses of 2D and 3D elastodynamic problems. The EDM inherits the excellent performance of FEM in the differentiation of the shape functions of isoparametric element to characterize the geometry and physical variables. The system equations of the dynamic problems directly established without using any variational principles or energy principles which generally are used in Galerkin finite element methods. As a consequence, no integrals are involved to form the coefficients of the system equations, and the EDM can be implemented easily for the dynamic problems.

The EDM method is a type of strong form numerical technique, which takes the advantages from the collocation method and FEM, giving a highly accurate strong formulation-based technique with the adaptability of finite elements. The EDM has the advantages of easy use in collocation method and can use the standard finite element meshes to handle geometrically complex configurations, and can achieve stable results as FEM.

The EDM can be easily extended to solve free and forced dynamic problems. Although the final stiffness matrices of the dynamic system are not symmetric, the system coefficient matrix is sparse. At the same

time, the dynamic equilibrium equations are collocated only at the internal nodes of the elements. The mass terms (mass density) only exist at the internal nodes. Thus, the consistent mass matrix of the EDM is diagonal, which will open the door for fully explicit time integration schemes.

In summary, for the free and forced vibration analyses the EDM can significantly reduce formulation and assembly effort with respect to FEM, while achieving the same level of accuracy and convergence rate. In view of the above advantages, it is worth to apply EDM to simulate more complex problems, such as the earthquake, high speed impact problems.

Acknowledgments

The supports of the National Natural Science Foundation (11772083, 11672061, 11572075), the Fundamental Research Funds for the Central Universities (DUT17LK26), and Dalian High Level Talent Innovation Support Program (2015R046) are gratefully acknowledged.

References

- [1] Zheng BJ, Gao XW, Zhang C. Radial integration BEM for vibration analysis of two- and three-dimensional elasticity structures.. *Appl Math Comput* 2016;277:111–26.
- [2] Viola E, Tornabene F, Fantuzzi N. Generalized differential quadrature finite element method for cracked composite structures of arbitrary shape. *Compos Struct* 2013;106:815–34.
- [3] Jing L, Ming P, Zhang W, Fu L, Cao Y. Static and free vibration analysis of functionally graded beams by combination Timoshenko theory and finite volume method. *Compos Struct* 2016;138:192–213.
- [4] Cotterell JA, Reali A, Bazilevs Y, Hughes TJR. Isogeometric analysis of structural vibrations. *Comput Methods Appl Mech Eng* 2006;195:5257–96.
- [5] Schillinger D, Evans JA, Frischmann F, René R, Hsu M, Hughes TJR. A collocated C0 finite element method: reduced quadrature perspective, cost comparison with standard finite elements, and explicit structural dynamics. *Int J Numer Methods Eng* 2015;102:576–631.
- [6] Wang Q, Choe K, Shi D, Sin K. Vibration analysis of the coupled doubly-curved revolution shell structures by using Jacobi-Ritz method. *Int J Mech Sci* 2018;135:517–31.

- [7] Li R, Wang P, Xue R, Guo X. New analytic solutions for free vibration of rectangular thick plates with an edge free. *Int J Mech Sci* 2017;131–132:179–90.
- [8] Chen D, Yang J, Kitipornchai S. Free and forced vibrations of shear deformable functionally graded porous beams. *Int J Mech Sci* 2016;108–109:14–22.
- [9] Hughes TJR. The finite element method: linear static and dynamic finite element analysis. New Jersey: Prentice-Hall; 1987.
- [10] Gao XW. An effective method for numerical evaluation of general 2D and 3D high order singular boundary integrals. *Comput Methods Appl Mech Eng* 2010;199(45):2856–64.
- [11] Yang L, Quan X, Cheng P, Cheng Z. A free energy model and availability analysis for onset of condensation on rigid and liquid surfaces in moist air. *Int J Heat Mass Transfer* 2014;78(7):460–7.
- [12] Khater AH, Temsah RS, Hassan MM. A Chebyshev spectral collocation method for solving Burgers' type equations.. *J Comput Appl Math* 2008;222(2):333–50.
- [13] Cui M, Duan W, Gao XW. A new inverse analysis method based on a relaxation factor optimization technique for solving transient nonlinear inverse heat conduction problems. *Int J Heat Mass Transfer* 2015;90:491–8.
- [14] Tornabene F, Fantuzzi N, Bacciochi M. The local GDQ method applied to general higher-order theories of doubly-curved laminated composite shells and panels: the free vibration analysis. *Compos Struct* 2014;116:637–60.
- [15] Bert C, Malik M. Differential quadrature method in computational mechanics. *Appl Mech Rev* 1996;49:1–27.
- [16] Shu C. Differential quadrature and its application in engineering. London: Springer; 2000.
- [17] Tornabene F, Viola E, Inman DJ. 2-D differential quadrature solution for vibration analysis of functionally graded conical, cylindrical and annular shell structures. *J Sound Vib* 2009;328:259–90.
- [18] Andakhshideh A, Maleki S, Aghdam MM. Non-linear bending analysis of laminated sector plates using generalized differential quadrature. *Compos Struct* 2010;92:2258–64.
- [19] Reali A, Hughes TJR. An introduction to isogeometric collocation methods.. In: Iso-geometric methods for numerical simulation. Springer; 2015. p. 173–204.
- [20] Models M, Auricchio F, Hughes TJR, Reali A, Sangalli G. Isogeometric collocation methods. *Math Model Methods Appl Sci* 2010;20:2075–107.
- [21] Kiendl J, Auricchio F, Beir L, Lovadina C, Reali A. Isogeometric collocation methods for the Reissner-Mindlin plate problem. *Comput Methods Appl Mech Eng* 2015;284:489–507.
- [22] Reali DAA, Auricchio F. Modified finite particle methods for stokes problems. *Comput Part Mech* 2018;5:141–60.
- [23] Asprone D, Auricchio F, Montanino A, Reali A. A modified finite particle method: multidimensional elasto-statics and dynamics. *Int J Numer Methods Eng* 2014;99:1–25.
- [24] Wang DD,, Wang J, Wu J. Superconvergent gradient smoothing meshfree collocation method. *Comput Methods Appl Mech Eng* 2018;340:728–66.
- [25] Fantuzzi N. New insights into the strong formulation finite element method for solving elastostatic and elastodynamic problems. *Curved and Layer Struct* 2014;1:93–126.
- [26] Fantuzzi N, Tornabene F, Viola E. Four-parameter functionally graded cracked plates of arbitrary shape: a GDQFEM solution for free vibrations. *Mech Adv Mater Struct* 2016;23(1):89–107.
- [27] Striz AG, Chen WI, Bert CW. Static analysis of structures by the quadrature element method (QEM). *Int J Solids Struct* 1994;31:2807–18.
- [28] Wen PH, Cao P, Korakianitis T. Finite block method in elasticity. *Eng Anal Bound Elem* 2014;46:116–25.
- [29] Li M, Wen PH. Finite block method for transient heat conduction analysis in functionally graded media. *Int J Numer Method Eng* 2014;99(5):372–90.
- [30] Fantuzzi N, Della Puppa G, Tornabene F, Trautz M. Strong formulation isogeometric analysis for the vibration of thin membranes of general shape. *Int J Mech Sci* 2017;120:322–40.
- [31] Gao XW, Huang SZ, Cui M, Ruan B, Zhu QH, Yang K, Lv J, Peng HF. Element differential method for solving general heat conduction problems. *Int J Heat Mass Transfer* 2017;115:882–94.
- [32] Gao XW, Li ZY, Yang K, Lv J, Peng HF, Cui M, Ruan B, Zhu QH. Element differential method and its application in thermal-mechanical problems. *Int J Numer Methods Eng* 2018;113(1):82–108.
- [33] Singiresu SR. Mechanical vibrations. Singapore: Prentice Hall; 2005.
- [34] Allan FB. Applied mechanics of solids. London: Taylor and Francis; 2009.
- [35] Brebbia CA, Telles JC, Wrobel LC. Boundary element techniques. Berlin: Springer-Verlag; 1984.
- [36] Gu YT, Liu GR. A meshless local Petrov–Galerkin (MLPG) method for free and forced vibration analysis for solids. *Comput Mech* 2001;27:188–98.
- [37] Shivanian E. A new spectral meshless radial point interpolation (SMRPI) method: a well-behaved alternative to the meshless weak forms. *Eng Anal Bound Elem* 2015;54:1–12.